IRAQI BULLETIN OF GEOLOGY AND MINING (IBGM)\
IRAQ GEOLOGICAL SURVEY (GEOSURV-IRAQ)

*IBGM (**2025**, Vol 21; Issue 2)* *321-333*

HEALTH RISK ASSESSMENT OF HEAVY METALS AND PHYSICOCHEMICAL PARAMETERS IN DUST FALLING ON SOME SELECTED AREAS OF BAGHDAD IN 2024

Huda Hadi Jassim[1], Raad Mahmoud Nasif Al-Khafaji[2*], Hasan Kattoof Jasim[3], and Adnan Jassam Humadi[4]

[1] Ministry of Education4Balqes Secondary School, Al.Rusafa 2, Baghdad, Iraq; huda.hadi2202@ihcoedu.uobaghdad.edu.iq.
[2] College of Education for Pure Sciences (Ibn Al-Haitham), University of Baghdad, Baghdad, Iraq; raad.m.n@ihcoedu.uobaghdad.edu.iq.
[3] College of Science - University of Baghdad, Baghdad, Iraq; hasan.jasim@sc.uobaghdad.edu.iq
[4] College of Education, Al- Al-Iraqia University, Baghdad, Iraq; adnan.h.humadi@aliraqia.edu.iq.
***** Correspondence: raad.m.n@ihcoedu.uobaghdad.edu.iq; Raad Mahmoud Nasif Al-Khafaji.

Type of the Paper (Article)
Received: 01/01/2025
Accepted: 25/08/2025
Available online: 27/12/2025

Abstract

Some dust storms that blew over the city of Baghdad in April 2024 were investigated in some locations and the following results were obtained: Volumetric analysis of the dust texture revealed a silt content of 42.4 – 58.6 % at 49%, a clay content of 29.5 – 55.1 % at 43%, a sand content of 7.9 – 12.4 % at 10%, a pH of 7.1 – 7.5 at an average of 8, ranging from neutral to relatively low alkalinity, an organic matter content of 1.22 – 1.83 % at an average of 2%, which is assumed to contain a high proportion of humic organic matter, and a percentage loss on ignition of 11.43 – 67.17 % at an average of 15%. It is hypothesised that the reason for this is the presence of various materials with a high proportion of calcium oxides and sulphates, and the presence of a low proportion of silica materials. The percentage of total dissolved salts is 511 parts per million - 748 parts per million, at an average of 619 ppm. The difference in values is probably due to the speed and direction of the wind carrying the dust. The Hazard Index (HI) is in descending order Chromium> Arsenic> Cobalt> Lead> Nickel> Zinc for adults and Cr>Co>Ni>As>Pb>Zn for children, while the CR and TCR values are in descending order Ni>Cr>As>Pb>Co for adults and Cr>Ni>As>Pb>Co for children.

Keywords: Physicochemical parameters; The risks; Dust storms; Heavy elements; Carcinogenic risks.

1. Introduction

Dust storms that blow across Iraq originate from both local and regional sources, with the latter arising from areas such as North Africa and the Middle East (Al-Dabbas & Al-Khafaji, 2012). Storms of any kind have detrimental effects on human health and society (Al-Dabbas

ISSN 1811-4539, EISSN 3005-3714
https://doi.org/10.59150/ibgm2102a16
IBGM: http://ibgm-iq.org/
Academic Scientific Journals: www.iasj.net

et al., 2012). In recent years, Baghdad has experienced a decline in green spaces and reforestation efforts, making the city increasingly vulnerable to the impacts of dust storms, which have become more frequent. The dust storms affecting Baghdad represent a significant natural hazard, often persisting for several days during specific months, particularly in spring and summer, and stemming from both regional and local sources (Jassim, 2021). Dust refers to particulate matter suspended in the atmosphere, typically with diameters up to 1000 micrometers, and is considered one of the major air pollutants, alongside sulfur dioxide, ozone, and lead. When deposited on agricultural fields, dust can be harmful to crops due to its content of heavy metals and other pollutants that negatively affect plant health.

Dust particles affect human life and health by reducing air quality in the study area. Numerous studies, including those by Al-Dabbas et al. (2011), have shown that dust storms carry various microorganisms that directly impact human health, causing illnesses such as allergies, asthma, and other conditions, including pollen- and fungus-related diseases.

Sultan et al. (2012) reported in their study of toxic and carcinogenic element concentrations in the dust and soil of Baghdad and Ramadi that some elements in suspended particles exceeded permissible concentration limits, while most other elements remained within acceptable ranges. Major atmospheric pollutants have been identified, such as lead from leaded gasoline, and copper, zinc, and cadmium originating from automotive parts, tire wear, lubricants, industrial emissions, and combustion sources (Willers et al., 2005; AL-Rasoul et al., 2012).

This research aims to investigate the sizes of the particles or fines that constitute the dust, as the size of these particles is closely related to the degree of environmental risk they pose.

2. Materials and methods

2.1. Location of the study area

Baghdad is the capital of the Republic of Iraq, located in the central part of the country between latitudes 33º10′ and 33º29′N, and longitudes 44º09′ and 44º33′E. The city's area is approximately 1,350 km². The Tigris River flows through Baghdad from north to south, dividing it into two main parts: Karkh and Rusafa. Baghdad represents about 1.04% of Iraq's total area (Table 1 and Figure 1).

Table 1. Geographic coordinates of the study area in which samples were collected for some storms that hit Baghdad in 2024.

Station No	Quarter Mane	Location	Altitude	Latitude
1	Hay Ur	North West	33 41 14 N	44 41 09 E
2	Al-Mashtal	South East	33 33 01 N	44 49 94 E
3	Hay Al-Shabab	South west	33 14 29 N	44 20 36 E

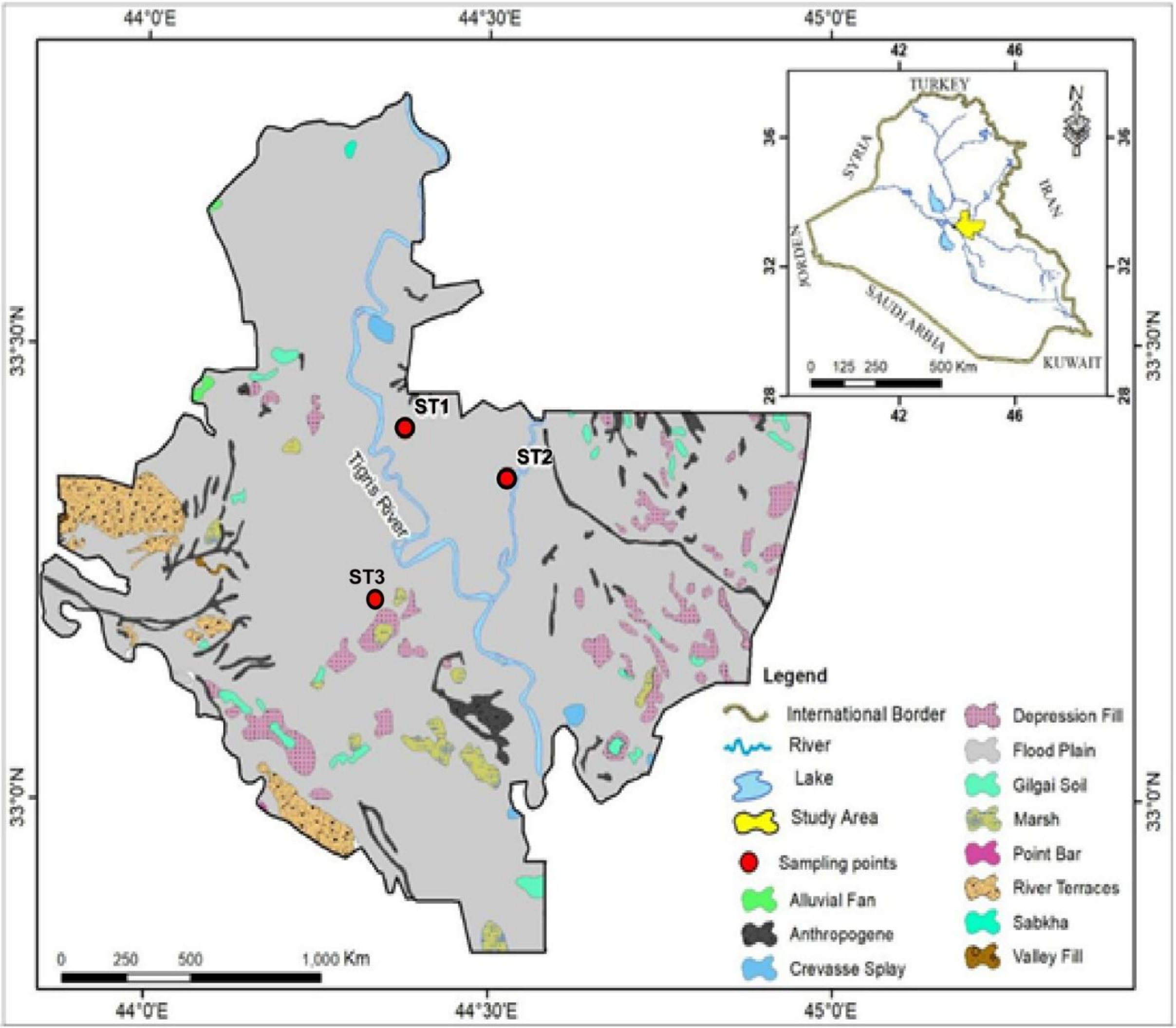

Figure 1. The study area's location.

2.2. Geology of the study area

The study area is primarily composed of Quaternary sediments, particularly those from the Pleistocene and Holocene epochs. These sediments mainly consist of silty clay interbedded with thin layers of sand and silt. While their age is attributed to the Holocene, it is believed that their formation began during the early Pleistocene. Alluvial deposits are the most widespread sediments in the study area, representing the main Holocene sedimentation cycle of the Mesopotamian Basin.

2.3. Dust samples

The method used to collect samples during dust storms involved spreading a layer of nylon over elevated areas of tall buildings, which served as sampling stations (Menéndez et al., 2007). An area of one square meter was covered with nylon to capture the falling dust. The duration of sample collection corresponded to the length of each storm and continued until its end. Samples were collected from rooftops located more than 3 meters above the ground surface. Dust samples were obtained between April 12 and April 28, 2024, from several areas in Baghdad, during which three dust storms occurred (Figure 1). Three local sampling stations were established in Baghdad Governorate, and the sampling locations were selected based on the details provided in Table 1.

3. Results and Discussion

3.1. Composition of the dust samples

The dust composition in the study areas of Baghdad is primarily clay (minimum = 29.5%, maximum = 55.1%, average = 43%), silt (minimum = 42.4%, maximum = 58.6%, average = 49%), and sand (minimum = 7.9%, maximum = 12.4%, average = 10%), according to the Folk (1974) classification system (Table 2 and Figure 2). The results of particle size distribution, when plotted on the Al-Ali (2003) triangular diagram, indicate that the majority of the dust texture is classified as silt, with smaller proportions of sandy silt. The high silt content is attributed to wind energy during the dry season, which contributes to the formation of dust storms. These findings align with previous studies that have shown dust storm sediments in Iraq are mainly composed of silt and clay with minor sand content. The variability in these components is influenced by wind speed and energy, which control the transport of particles smaller than 63 microns during the dry season. The results are consistent with those reported by Kamble (1995), Al-Ali et al. (2005), and ROPME (2016), who emphasized that the texture of dust in Iraqi storms is predominantly silt and clay, with particle composition varying according to wind dynamics and transport capacity.

Table 2. Grain Size Analysis of dust storms in Baghdad – April/ 2024.

City	Date of Storm	Station Number	Location of Stations	Sand %	Silt %	Clay %	Type of texture According to Folk (1974)
		1	North	7.7	43.8	48.5	Mud
	8/4/2024	2	South East	7.9	42.4	49.7	Mud
		3	South West	8.4	46.5	55.1	Mud
		1	North	7.9	49.2	42.9	Mud
Baghdad	15/4/2024	2	South East	9.6	49.9	40.5	Mud
		3	South West	8.8	45.5	45.7	Mud
		1	North	10.5	52.2	37.3	Sandy mud
	28/4/2024	2	South East	11.9	58.6	29.5	Sandy mud
		3	South West	12.4	49.5	38.1	Sandy mud
Min.				7.9	42.4	29.5	
Mix.				12.4	58.6	55.1	
Mean				10	49	43	

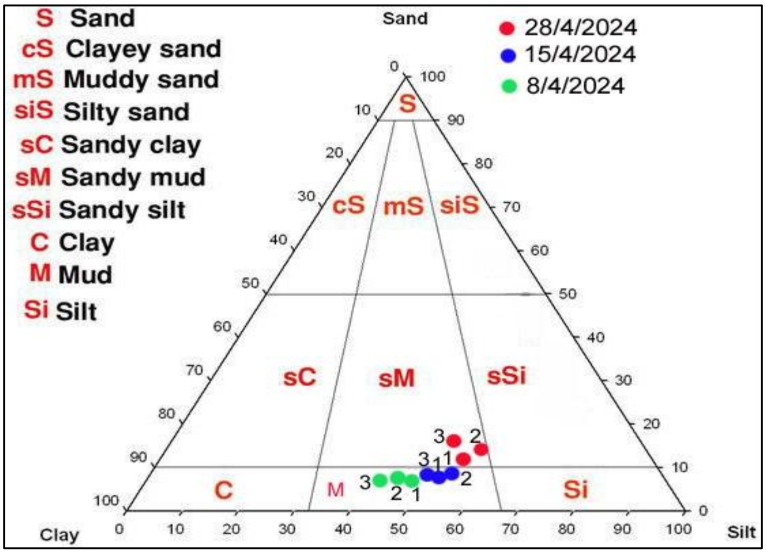

Figure 2. Dust samples of the study area were plotted on the (Folk, 1974).

3.2. pH Value

The results obtained show that the pH values, as presented in Table 3, range from 7.1 to 7.5, indicating that the samples are slightly to moderately alkaline.

3.3. Organic matter (OM)

Table (3) shows that the lowest value is 1.22%, the highest is 1.83%, with an average of approximately 2%.

Table 3. Physical properties of the study area samples.

City	Date of Storm	Station Number	Location	Organic Matters %	pH	TDS ppm	L.O.I
		1	North	1.43	7.1	513	12.44
	8/4/2024	2	South East	1.52	7.3	511	15.37
		3	South West	1.57	7.2	547	13.35
		1	North	1.51	7.4	548	16.65
Baghdad	15/4/2024	2	South East	1.83	7.5	599	17.76
		3	South West	1.46	7.1	657	15.36
		1	North	1.22	7.2	748	11.43
	28/4/2024	2	South East	1.43	7.3	699	15.57
		3	South West	1.15	7.3	746	14.42
Min				1.22	7.1	511	11.43
Mix				1.83	7.5	748	17.76
Mean				2	8	618.7	15

3.4. Loss of Ignition (L.O.I)

The percentage of loss on ignition (LOI) for the samples from the study area, as shown in Table 3, ranges between 11.43% and 67.17%, with an average of 15%. This may be attributed to the high content of calcium oxide and sulfates, and the low content of silica.

3.5. Total Dissolved Salts (TDS)

The analytical results of the dust samples, as presented in Table 3, indicate that the values of total dissolved salts range from 511 ppm to 748 ppm, with an average of 618.7 ppm. The variation in these values may be attributed to wind speed and direction, which influence the quantity of dust transported and deposited. In the absence of wind, dust deposition tends to decrease. It is assumed that the source of these dissolved salts in dust storms originates either from source rock areas that have undergone weathering processes (Al-Zubaidi, 2020) or from the transport of soil during storms from various regions, including agricultural and non-agricultural lands. When comparing the pH values in the study area with the soil classification in Table 4, it is evident that the dust samples are not saline, as the pH values remain below 8.5.

Table 4. Soil classification according to salinity in the United States Salinity Laboratory in USEPA (2017).

Soil type	**Soil reaction pH value**
Non-saline soil	8.5 <
alkaline soil	8.5 >

3.6. Health risk assessment model

The average daily dose (ADD) of each analyzed trace element via ingestion, inhalation, and dermal contact was calculated using Equations (1), (2), and (3) (USEPA, 2017; Gabarron et al., 2017).

$$ADD_{ingestion} = \frac{C \cdot Ring \cdot EF \cdot ED \cdot 1.0E\text{-}6}{BW \cdot AT} \quad (1)$$

$$ADD_{inhalation} = \frac{C \cdot Rinh \cdot EF \cdot ED}{PEF \cdot BW \cdot AT} \quad (2)$$

$$ADD_{dermal} = \frac{C \cdot SA \cdot SL \cdot ED \cdot EF \cdot ABS \cdot 1.0E\text{-}6}{BW \cdot AT} \quad (3)$$

ADD values refer to the average daily absorption of each trace element through ingestion, inhalation, and dermal contact, expressed in units of mg/kg·day. Table 5 presents the exposure factors used in the dose models (USEPA, 2002; Gabarrón et al., 2017; Qadeer et al., 2020; Tables 5 and 6).

Table 5. exposure factors for dose models (USEPA, 2002; Gabarrón et al., 2017; Qadeer et al., 2020).

Items	Parameter	Definition	Units	Adults	Children
Basic parameters	C	Heavy metal concentration	Ppm	The current study (Table 7)	
	CF	Conversion factor	Kg/mg	$1 * 10^{-6}$	$1 * 10^{-6}$
Exposure behavioral parameters	EF	exposure Frequency	Day/year	350	350
	ED	Exposure duration	in a year	24	6
	BW	Body weight	Kg	55.9	15
	AT	Average Time –non carcinogen	Days	365×ED	365×ED
		Average time of carcinogens	Days	365*70	365*70
Digestive tract/ inhalation	R_{ing}	Ingestion rate	Mg/Kg	100	200
	R_{inh}	Inhalation rate	M^3 /Kg	20	5
	PEF	Particle emission factor	M^3 /Kg	1.32×10^9	1.32×10^9
Skin contact	SA or AF	skin surface area	Cm^2	5000	1800
	SL	Skin adherence factor	mg/cm^2	1	1
	ABS (R_{derm})	Dermal absorption	Unit less	0.001	0.001

Table 6. Average concentrations of elements for three times (in ppm).

	V	Cr	Co	Ni	Zn	As	Cd	Pb
North	191	429	20	218	106	11.8	2	12.5
SE	204	677	23	229	100	10.4	2	11.5
SW	201	401	20	243	97	11.3	2	11.4

3.6.1. Assessment of non-carcinogenic risks

The non-cancer risk was assessed using the hazard quotient (HQ) for each trace element by dividing the ADD calculated from Equations (1), (2), and (3) by the reference dose (RfD) (EPA, 1989), as shown in Equation (4).

$$HQ= ADD/RFD \tag{4}$$

HQ > 1 indicates a potential for adverse health effects, while HQ < 1 suggests no expected health risk (Chonokhuu *et al.*, 2019). The hazard index (HI) was then calculated by summing the HQ values from the three exposure pathways for each corresponding element (Zgłobicki & Telecka, 2021), as described by Equation (5).

$$HI=\int HQ \tag{5}$$

If the HI value is less than 1, it indicates a very low risk; an HI between 1 and 4 suggests possible risk effects, while an HI greater than 4 indicates a high risk (Tan et al., 2021) (Table 7).

Table 7. Reference dose for non-cancer risks and slope factors for cancer risks assessment.

El.	RFD_{ing}	RFD_{inh}	RFD_{derm}	SF_{ing}	SF_{inh}	SF_{derm}	**Refere.**
As	$3.0 * 10^{-4}$	$3.0 * 10^{-4}$	$1.2 * 10^{-4}$	$1.5 * 10^{0}$	$1.51 * 10^{1}$	$3.66 * 10^{0}$	(USEPA, 2009; Tan *et al.*, 2021)
Co	$3.0 * 10^{-4}$	$2.0 * 10^{-2}$	$5.4 * 10^{-3}$	--	$8.4 * 10^{-1}$	--	(USEPA, 2009; Gabarron *et al.* 2017)
Cr	$3.0 * 10^{-3}$	$2.86 * 10^{-6}$	$6.0 * 10^{-5}$	$5.0 * 10^{-1}$	$4.1 * 10^{-1}$	--	(Gabarron *et al.*, 2017*;* Tan *et al.*, 2021)
Ni	$1.1 * 10^{-2}$	$6.0 * 10^{-6}$	$1.6 * 10^{-2}$	$1.7 * 10^{0}$	$9.8 * 10^{0}$	--	(USEPA, 2009; USEPA, 2017)
Pb	$3.5 * 10^{-3}$	$3.5 * 10^{-3}$	$5.25 * 10^{-4}$	$8.5 * 10^{-3}$	$4.2 * 10^{-2}$	--	(Gabarron *et al.*, 2017*;* Tan *et al.*, 2021)
Zn	$3.0 * 10^{-1}$	$3.0 * 10^{-1}$	$6.0 * 10^{-2}$	--	--	--	(Gabarron *et al.*, 2017*;* USEPA, 2021)

The study indicates a higher non-cancer risk (HI > 1) for chromium (Cr) in both children and adults (Figure 3). When considering the average hazard index across the three sites (N, SE, and SW), the data reveal a non-cancer risk for children associated with the trace elements arsenic (As) and lead (Pb; Table 8, Figure 4). Chromium was the only element consistently associated with a non-cancer risk across all groups. These findings suggest a potential non-carcinogenic health risk for children in the study area, primarily through ingestion and dermal contact. This is particularly concerning, as children frequently play in dust and often put their fingers or hands in their mouths during play.

3.6.2. Assessment of the carcinogenic risk (CR)

After calculating the average daily dose (ADD) for each exposure pathway, the carcinogenic risk (CR) was determined by multiplying the ADD by the corresponding slope factor (SF), as recommended by the USEPA (2016), using Equation (6).

$$CR= ADD \times SF \tag{6}$$

The total cancer risk (TCR) is calculated as the sum of the carcinogenic risks (CR) from the three exposure pathways (Shabbaj et al., 2018), using Equation (7).

$$TCR=\int CR \quad (7)$$

Table 8. HQ and HI values for the elements in the dust of the study area.

Metals	Pathway	North		South East		South West	
		Adults	Children	Adults	Children	Adults	Children
Arsenic	HQ_{ing}	$6.74 * 10^{-1}$	$5.02 * 10^{-2}$	$5.94 * 10^{-2}$	$4.43 * 10^{-1}$	$6.46 * 10^{-2}$	$4.82 * 10^{-1}$
	HQ_{inh}	$1.02 * 10^{-5}$	$1.71 * 10^{-4}$	$9.01 * 10^{-6}$	$5.23 * 10^{-5}$	$9.78 * 10^{-6}$	$5.47 * 10^{-5}$
	HQ_{derm}	$3.51 * 10^{-4}$	$1.96 * 10^{-4}$	$3.09 * 10^{-4}$	$1.80 * 10^{-3}$	$3.64 * 10^{-3}$	$1.88 * 10^{-3}$
	HI	$6.75 * 10^{-1}$	$5.06 * 10^{-2}$	$5.97 * 10^{-2}$	$4.45 * 10^{-1}$	$6.79 * 10^{-2}$	$4.84 * 10^{0}$
Lead	HQ_{ing}	$6.12 * 10^{-2}$	$4.5 * 10^{-2}$	$5.63 * 10^{-3}$	$4.20 * 10^{0}$	$5.58 * 10^{-3}$	$4.16 * 10^{-2}$
	HQ_{inh}	$9.28 * 10^{-7}$	$5.18 * 10^{-6}$	$8.53 * 10^{-7}$	$4.77 * 10^{-6}$	$9.87 * 10^{-7}$	$4.73 * 10^{-6}$
	HQ_{derm}	$8.50 * 10^{-5}$	$4.76 * 10^{-4}$	$7.82 * 10^{-5}$	$4.38 * 10^{-1}$	$3.32 * 10^{-4}$	$4.38 * 10^{-4}$
	HI	$6.13 * 10^{-2}$	$4.61 * 10^{-2}$	$5.71 * 10^{-3}$	$4.6 * 10^{0}$	$5.91 * 10^{-3}$	$4.20 * 10^{-2}$
Cobalt	HQ_{ing}	$1.14 * 10^{-1}$	$8.52 * 10^{-1}$	$1.31 * 10^{-1}$	$9.80 * 10^{-1}$	$1.14 * 10^{-1}$	$8.52 * 10^{-1}$
	HQ_{inh}	$2.59 * 10^{-2}$	$1.45 * 10^{-6}$	$2.98 * 10^{-7}$	$1.67 * 10^{-6}$	$2.59 * 10^{-2}$	$1.45 * 10^{-6}$
	HQ_{derm}	$1.32 * 10^{-5}$	$7.40 * 10^{-5}$	$1.52 * 10^{-5}$	$8.51 * 10^{-4}$	$1.32 * 10^{-5}$	$7.40 * 10^{-5}$
	HI	$1.40 * 10^{-1}$	$8.52 * 10^{-1}$	$1.31 * 10^{-1}$	$9.80 * 10^{-1}$	$1.4 * 10^{-1}$	$8.52 * 10^{-1}$
Zinc	HQ_{ing}	$6.06 * 10^{-4}$	$4.51 * 10^{-3}$	$5.71 * 10^{-4}$	$4.26 * 10^{-3}$	$5.54 * 10^{-4}$	$4.13 * 10^{-3}$
	HQ_{inh}	$9.18 * 10^{-8}$	$5.13 * 10^{-7}$	$8.66 * 10^{-8}$	$4.84 * 10^{-7}$	$8.40 * 10^{-8}$	$4.69 * 10^{-7}$
	HQ_{derm}	$6.31 * 10^{-6}$	$3.53 * 10^{-5}$	$5.95 * 10^{-6}$	$3.33 * 10^{-5}$	$5.77 * 10^{-6}$	$3.23 * 10^{-5}$
	HI	$6.12 * 10^{-4}$	$4.55 * 10^{-3}$	$5.77 * 10^{-4}$	$4.29 * 10^{-3}$	$5.60 * 10^{-4}$	$4.16 * 10^{-3}$
Nickel	HQ_{ing}	$3.39 * 10^{-2}$	$2.53 * 10^{-1}$	$3.57 * 10^{-2}$	$2.66 * 10^{-1}$	$3.78 * 10^{-2}$	$2.82 * 10^{-1}$
	HQ_{inh}	$9.44 * 10^{-3}$	$5.27 * 10^{-2}$	$9.91 * 10^{-3}$	$5.54 * 10^{-2}$	$1.05 * 10^{-2}$	$5.88 * 10^{-2}$
	HQ_{derm}	$4.86 * 10^{-5}$	$2.72 * 10^{-4}$	$2.86 * 10^{-4}$	$2.86 * 10^{-4}$	$5.42 * 10^{-6}$	$3.03 * 10^{-4}$
	HI	$4.34 * 10^{-2}$	$3.06 * 10^{-1}$	$4.59 * 10^{-2}$	$3.21 * 10^{-1}$	$4.84 * 10^{-2}$	$3.41 * 10^{-1}$
Chromium	HQ_{ing}	$2.45 * 10^{-1}$	$1.82 * 10^{0}$	$3.87 * 10^{-1}$	$2.88 * 10^{0}$	$2.29 * 10^{-1}$	$1.70 * 10^{0}$
	HQ_{inh}	$3.71 * 10^{-5}$	$2.07 * 10^{-4}$	$5.86 * 10^{-5}$	$3.27 * 10^{-4}$	$3.47 * 10^{-5}$	$1.94 * 10^{-4}$
	HQ_{derm}	$5.72 * 10^{-1}$	$3.00 * 10^{0}$	$8.45 * 10^{-1}$	$5.05 * 10^{0}$	$5.01 * 10^{-1}$	$2.80 * 10^{0}$
	HI	$8.17 * 10^{-1}$	$4.82 * 10^{0}$	$1.23 * 10^{0}$	$7.93 * 10^{0}$	$7.30 * 10^{-1}$	$4.51 * 10^{0}$

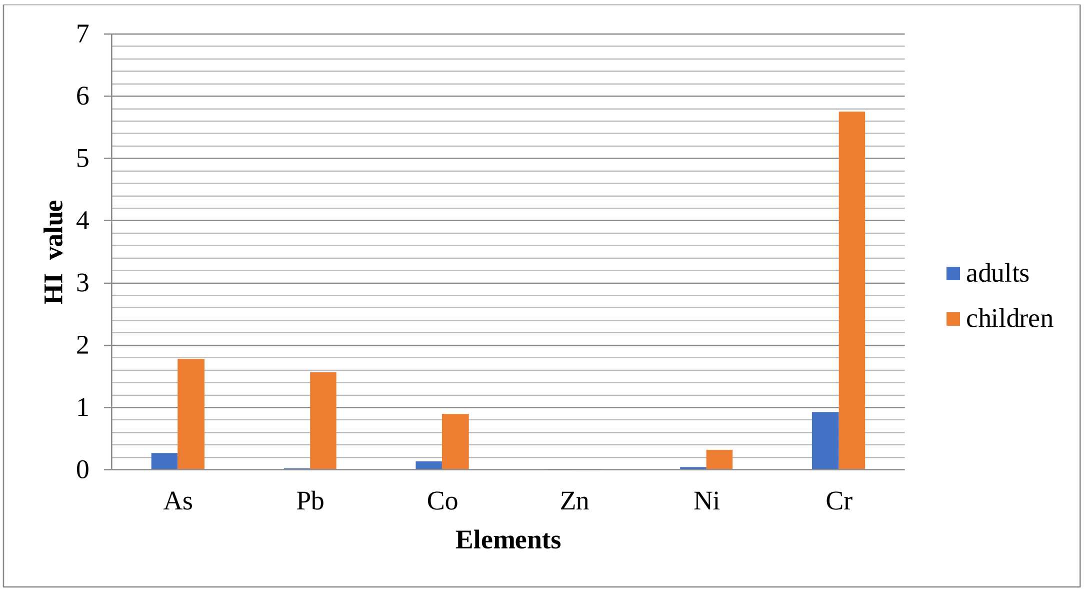

Figure 3. Contribution of elements to non-cancer risk.

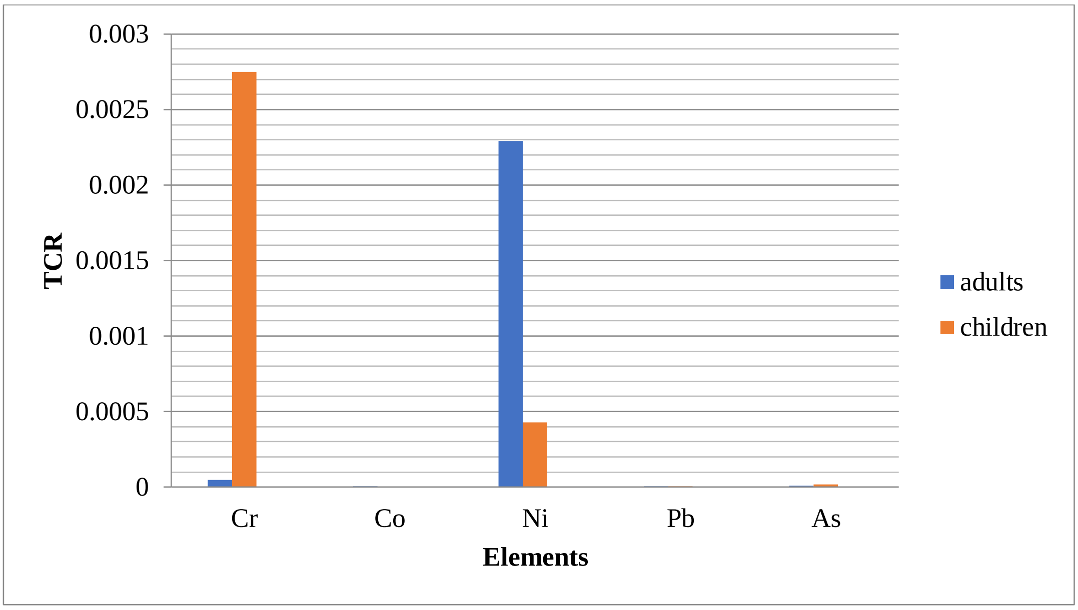

Figure 4. Contribution of elements to cancer risk.

The tolerable risk level is generally considered to fall within the range of 10^{-6} to 10^{-4}. Risks are classified as follows: very low ($<10^{-6}$), low (10^{-6} – 10^{-5}), medium (10^{-5} – 10^{-4}), high (10^{-4} – 10^{-3}), and very high ($>10^{-3}$) (USEPA, 2016). This study indicates that nickel (Ni) poses a carcinogenic risk for adults, with a TCR value greater than 1.0×10^{-4}, while chromium (Cr) presents a carcinogenic risk for children (Figure 4). The findings also suggest a possible carcinogenic risk (TCR between 1.0×10^{-6} and 1.0×10^{-4}) from Ni, arsenic (As), and lead (Pb) for children, and a potential risk from Cr for adults. Moreover, the study shows no carcinogenic risk associated with cobalt (Co) and Pb for both adults and children. The descending order of CR and TCR values is as follows: For adults: Ni > Cr > As > Pb > Co. For children: Cr > Ni > As > Pb > Co (Table 9).

Table 9. CR and TCR for elements of the study area.

$Pathway/Metals$		Cr	Co	Ni	Pb	As
$CR/_{ing}$	Adult	$4.77 * 10^{-4}$	-----	$2.29 * 10^{-3}$	$5.89 * 10^{-8}$	$9.85 * 10^{-6}$
$CR/_{inh}$		$1.82 * 10^{-8}$	$1.57 * 10^{-9}$	$2.44 * 10^{-7}$	$4.41 * 10^{-11}$	$1.50 * 10^{-8}$
$CR/_{derm}$		$2.25 * 10^{-5}$	------	------	------	$5.00 * 10^{-8}$
TCR		$4.79 * 10^{-5}$	$1.57 * 10^{-9}$	$2.29 * 10^{-3}$	$5.89 * 10^{-8}$	$9.91 * 10^{-6}$
$CR/_{ing}$	Children	$2.75 * 10^{-4}$	------	$4.28 * 10^{-4}$	$1.09 * 10^{-7}$	$1.83 * 10^{-5}$
$CR/_{inh}$		$4.27 * 10^{-9}$	$3.66 * 10^{-10}$	$4.67 * 10^{-8}$	$1.02 * 10^{-11}$	$3.49 * 10^{-9}$
$CR/_{derm}$		$3.02 * 10^{-6}$	------	------	------	$6.71 * 10^{-8}$
TCR		$2.75 * 10^{-3}$	$3.66 * 10^{-10}$	$4.28 * 10^{-4}$	$1.09 * 10^{-7}$	$1.83 * 10^{-5}$

4. Conclusions

The pH value in the study area was found to range from moderate to alkaline. This alkalinity is attributed to the presence of alkaline chemical elements within the clay minerals that make up the transported dust, giving it an overall alkaline character. The origin of the organic matter, total dissolved salts, and other chemical compounds transported with the dust during storms in the study area is likely either from source rocks that have undergone weathering and become friable due to wind erosion, or from various anthropogenic sources such as agricultural and industrial wastes that are carried by wind from their source to the deposition area. The substances lost from the dust during the ignition process are primarily chemical compounds that contain water molecules, such as calcium oxides and sulfates. The hazard index (HI) was found to be less than one for all elements, indicating no significant non-carcinogenic risk for both children and adults—except for chromium (Cr), which showed an HI greater than one for children. In terms of carcinogenic risk, nickel (Ni), arsenic (As), and lead (Pb) pose potential risks for children, while chromium (Cr) poses a potential carcinogenic risk for adults. In this study, the hazard index (HI) values for adults, in descending order, were Cr > As > Co > Pb > Ni > Zn, and for children, Cr > Co > Ni > As > Pb > Zn. The carcinogenic risk (CR) and total cancer risk (TCR) values followed the order:

For adults: Ni > Cr > As > Pb > Co, For children: Cr > Ni > As > Pb > Co.

References

Al-Ali, J. T. (2003). Dust storms contribution of Khor al-Zubair and Khor Abdallah deposits. *Journal of the Iraqi Geographical Society*, *53*.

Al-Ali, J. T., Abdul Jabbar, C. H., & Hassan, H. (2005). Effect of Marshlands drying process on regional dust fallout. *Wade Al-Rafedian Magazine*, *16*, 261–272.

Al-Dabbas, M. A., Ayad Abbas, M., & Al-Khafaji, R. M. (2012). Dust storms loads analyses—Iraq. *Arabian Journal of Geosciences*, *5*(1), 121–131.

Al-Dabbas, M., Abbas, M. A., & Al-Khafaji, R. (2011). The mineralogical and micro-organisms effects of regional dust storms over Middle East region. *International Journal of Water Resources and Arid Environments*, *1*(2), 129–141.

Al-Dabbas, M., & Al-Khafaji, R. (2012). Some Geochemical, textural and radioactive characteristics of the sandstorms loads blown over Baghdad and Ramadi cities, Middle Iraq. *Iraqi Journal of Science*, *53*(Remote Sensing-Conf), 57–66.

AL-Rasoul, K., Ali, F., Jubair, S., Ali, Q., Najim, A., Hussain, M., & Ahmed, F. (2012). Deposition of Major and Trace Elements from the Atmosphere Over Baghdad During the Year 2010. *Iraqi Journal of Science*, *53*(Remote Sensing-Conf), 33–39.

Al-Zubaidi, A. H. (2020). *No Title* (2nd ed.). Dar Al-Hikma for Printing and Publishing.

Chonokhuu, S., Batbold, C., Chuluunpurev, B., Battsengel, E., Dorjsuren, B., & Byambaa, B. (2022). Contamination and health risk assessment of heavy metals in the soil of major cities in Mongolia. *International journal of environmental research and public health*, *16*(14), 2552. https://doi.org/10.3390/ijerph16142552.

Folk, R. (1974). Petrology of sedimentary rocks. Hamphill, Texas, 182pp.

Gabarrón, M., Faz, A., Martínez-Martínez, S., Zornoza, R., & Acosta, J. A. (2017). Assessment of metals behaviour in industrial soil using sequential extraction, multivariable analysis and a geostatistical approach. *Journal of Geochemical Exploration*, *172,* 174–183.

EPA, A. (1989). *Risk assessment guidance for superfund. Volume I: Human Health Evaluation Manual (part a)* (p. 205). EPA/540/1-89/002.

Jassim, H. H. (2021). *Ecological Geological Study of Street dust within some areas of Al-Rusafa/Baghdad City/Iraq*. MSc. thesis. College of Education for Pure Science/Ibn Al-Haitham ….

Kamble, S. T. (1995). *Fate of insecticides used for termite control in soil*. Cooperative Extension, Institute of Agriculture and Natural Resources ….

Menéndez, I., Díaz-Hernández, J. L., Mangas, J., Alonso, I., & Sánchez-Soto, P. J. (2007). Airborne dust accumulation and soil development in the North-East sector of Gran Canaria (Canary Islands, Spain). *Journal of Arid Environments*, *71*(1), 57–81.

Qadeer, A., Saqib, Z. A., Ajmal, Z., Xing, C., Khalil, S. K., Usman, M., Huang, Y., Bashir, S., Ahmad, Z., & Ahmed, S. (2020). Concentrations, pollution indices and health risk assessment of heavy metals in road dust from two urbanized cities of Pakistan: Comparing two sampling methods for heavy metals concentration. *Sustainable Cities and Society*, *53*, 101959.

ROPME. (2016). Dust fallout in the northern part of the. ROPME Arid, Final report of the Regional Organization for the Protection of the Marine Environment, Kuwait.

Shabbaj, I. I., Alghamdi, M. A., Shamy, M., Hassan, S. K., Alsharif, M. M., & Khoder, M. I. (2018). Risk assessment and implication of human exposure to road dust heavy metals in Jeddah, Saudi Arabia. *International Journal of Environmental Research and Public Health*, *15*(1), 36.

Sultan, M., Al-Rubaiee, M., & Abdulrahim, E. (2012). Assessment of toxic and carcinogenic elements in Dust and Soil in Baghdad city and their effects on the distribution of some diseases. *Iraqi Journal of Science*, *53*(Remote Sensing-Conf), 167–177.

Tan, B., Wang, H., Wang, X., Ma, C., Zhou, J., & Dai, X. (2021). Health risks and source analysis of heavy metal pollution from dust in Tianshui, China. *Minerals*, *11*(5), 502.

USEPA (United States Environmental Protection Agency). (2002). Supplemental Guidance for developing soil screening levels for superfund sites. Office of Emergency and Remedial Response. Washington, DC.2002.

USEPA (2009). Assessment Risk Guidance for superfund (Rags), Volume 1: Human Health Evaluation Manual (part E, Supplemental Guidance for dermal Risk Assessment) Interian.

U.S. Environmental Protection Agency. Washington, D.C. USEPA (2016). United States Environmental Protection Agency, Regional Screening Levels. *U.S. Environmental Protection Agency*. May 2016, prepared by Oak Ridge National Laboratories. Online available at: https://www.epa.gov/environmental-topics/chemicals-pesticides-and-toxics-topics.

USEPA (2017). United States Environmental Protection Agency, Regional Screening Level (RSL). Summary table. Online available at: https://www.epa.gov/risk/regional-screening-levels-rsls-generic-tables-june-2017

USEPA (2021). Regional Screening levels (RSLs). 2021.

Willers, S., Gerhardsson, L., & Lundh, T. (2005). Environmental tobacco smoke (ETS) exposure in children with asthma—relation between lead and cadmium, and cotinine concentrations in urine. *Respiratory Medicine*, *99*(12), 1521–1527.

Zgłobicki, W., & Telecka, M. (2021). Heavy metals in urban street dust: health risk assessment (Lublin City, E Poland). *Applied Sciences*, *11*(9), 4092.

About the author

Huda Hadi Jassim, Profession: Teacher at Al. Balqis Secondary School for Girls/Alrusafa /2 Ministry of Education. Academic Rank: Assistant Lecturer; Date of Master's Degree: 2021; Specialization: Biology. Master's thesis: (Geological environmental study of road dust in some areas of Russafa/Baghdad, Iraq), Research papers: 3 published research papers. Currently: PhD student in research phase.

e-mail: Huda.Hadi2202@ihcoedu.uobaghdad.edu.iq